ELSEVIER

Thin Solid Films 327–329 (1998) 185–190

thin solid films

Atomic force microscopic studies on the growth of self-assembled monolayers on $SrTiO_3$-surfaces

Boike L. Kropman*, Dave H.A. Blank, Horst Rogalla

Department of Applied Physics, University of Twente, P.O. Box 217, 7500 AE Enschede, The Netherlands

Abstract

The growth mechanism of octadecyltrichlorosilane (OTS) on $SrTiO_3$ substrates has been investigated by wettability and force microscopy measurements. The films were formed by the self-assembly technique. It was found that growth proceeded via two types of islands: large 'fractal-like' islands and smaller circular patches of molecules. The patches grow by attachment of monomers and coalescence with other islands. The overall growth mode obeyed first order Langmuir kinetics and is found to be similar to the growth of alkylsiloxanes on SiO_2 and mica. The difference between growth on $SrTiO_3$ and $SrTiO_3$:Nb is that the growth rate is slower on the latter substrate.

Keywords: Atomic force microscopy; Octadecylchlorosilane; Self-assembly

1. Introduction

Self-assembled monolayers (SAMs), formed by the spontaneous adsorption of amphiphiles on a number of different substrates [1,2], has proven to be a reliable and convenient way to form ultrathin organic films. $SrTiO_3$, like other perovskites, display a number of electrical effects (e.g. ferro- and piezoelectricity, giant magnetoresistance) and is used as a catalyst for the decomposition of water. By doping with niobium (Nb), the conductivity of the substrate can be varied from isolating to semiconducting. Furthermore, $SrTiO_3$ is used extensively as substrate for the deposition of high T_c superconducting $YBa_2Cu_3O_7$ films and related other perovskites [3], which explains the renewed interest in methods to obtain atomically smooth and chemically well-defined surfaces. We used $SrTiO_3$ and $SrTiO_3$:Nb as a model substrate for the formation of alkyltrichlorosilane SAMs on different perovskite surfaces, and to study its surface chemistry for the growth of superconducting materials.

During the past few years many reports have been devoted to the final film structure by various surface science techniques. However, some effort has lately been put in understanding the growth kinetics of alkylthiols on gold by wettability [4,5], second harmonic generation (SHG) [6], quartz crystal microbalance (QCM) [7], surface plasmon resonance (SPR) [8] and STM [9] measurements. Most studies conclude that there are at least two distinct steps in the kinetics: a fast step that can be described by Langmuir kinetics and a slower rearrangement step. Poirier and Pylant have also found that the growth rate is proportional to the unoccupied surface sites (first order Langmuir kinetics) in the case of gas-phase adsorption. First, the individual molecules form a mobile two dimensional lattice gas until complete coverage is reached, followed by the formation of dense crystalline islands (described as a lateral pressure-induced phase transformation). This process is completed if the surface is completely covered by such islands, leaving domains of molecules with different orientations with respect to the surface [9].

A few kinetic growth studies of other SAM-systems are available, e.g. in situ atomic force microscopy (AFM) on octadecylphosphonic acid/mica [10], AFM on alkyltrieth-oxysilane/mica [11] and AFM on alkyltrichlorosilanes on mica [12–14] and SiO_2 [15–18]. The general conclusion of these studies is that such SAMs form via an island growth mechanism. Individual molecules are highly mobile before final anchoring to the surface or cross-linking to neighbouring molecules occurs. Furthermore, there is a continuous exchange between adsorbed molecules and molecules in the solution (adsorption and desorption) before final anchoring takes place.

* Corresponding author. E-mail: b.l.kropman@tn.utwente.nl

0040-6090/98/$ - see front matter
PII S0040-6090(98)00625-7

In our previous work, a protocol has been established for the growth of a densely packed and organised monomolecular layer of alkyltrichlorosilane molecules on different $SrTiO_3$ substrates [19,20]. SAMs prepared by immersion for times longer than 2 h have been characterised extensively by ellipsometry, wettability, AFM, reflection absorption infrared spectroscopy (RAIRS) and angular resolved X-ray photoelectron spectroscopy (ARXPS). Ordered monomolecular films have been found with thicknesses of 2.4 nm comprised of densely packed and crystalline alkyl chains, tilted from the surface normal by 11° ($SrTiO_3$) or ~35° ($SrTiO_3$:Nb) [20]. The surface of the monolayer is composed of methyl groups, as evidenced by their high contact angles ($\theta_{adv}^{H_2O} > 110°$, $\theta_{adv}^{HD} > 40°$). Furthermore, it is concluded that a network of cross-linked siloxanes is formed just above the original surface, with only a small number of bonds to the $SrTiO_3$ [19] and a fused silica surface [21]. Regarding the formation of high-quality SAMs comprised of alkyltrichlorosilanes, it has been recognised that the temperature of the adsorption solution and humidity play a crucial role [22,23]. High-quality films can only be formed below a critical temperature T_c (which depends on the length of the alkyl chain and on the molecule itself); above this temperature less dense and less crystalline films are formed.

In this report, the formation of SAMs of octadecyltrichlorosilane on both $SrTiO_3$ and niobium-doped $SrTiO_3$ ($SrTiO_3$:Nb) are studied by wettability and atomic force measurements.

2. Experimental

Octadecyltrichlorosilane (OTS, 95%) and *n*-hexadecane (HD, 99% +) were obtained from Aldrich and used as received. $SrTiO_3$ and 0.05 wt.% doped $SrTiO_3$:Nb substrates (ESCETE, Enschede, The Netherlands) were cut within 0.2° of the (001)-direction and polished. For the water contact angles, filtered and deionised Millipore water (R = 15 MΩ) has been used.

Before adsorption took place, the $SrTiO_3$ substrates were cleaned ultrasonically in a sequence of solvents (chloroform, acetone and alcohol), followed by a short (1 min) immersion in dilute phosphoric acid [19]. Each series of adsorptions was carried out in a freshly prepared solution of ~1mM OTS in HD. The temperature and relative humidity (RH) during deposition are controlled as well as possible, i.e. the adsorption took place in a climate room ($T \leq 20$°C, RH 20–40%). The growth behaviour was studied by immersing the substrates for different periods of time in this solution (t = 0, 10 s, 1, 2, 3, 5 and 10 min, and 1 h). To remove physisorbed and/or complexed HD, the monolayer was sonicated several minutes in chloroform and ethanol. Immediately after adsorption, the films are characterised by their advancing contact angle with water ($\theta_{adv}^{H_2O}$), atomic force microscopy (AFM) and lateral force microscopy (LFM).

Contact angles have been measured on several locations on the sample. All results were averaged and the accuracy obtained by this method is approximately ±3°. AFM and LFM measurements were performed in the contact mode on a Nanoscope IIIa (Digital Instruments). Cantilevers (supplied by Digital Instruments) with different nominal force constants (k_N (k_{tors}) = 0.08, 0.18, 0.38 (80) or 0.58 (175) N/m [24]) were used. Forces are measured by the displacement of the reflected spot of a laser beam from the backside of a cantilever on a position sensitive quadrant detector. Normal forces (F_N) induce bending of the cantilever and result in a vertical movement of the spot, whereas frictional forces (F_f) exert a torque on the cantilever which results in horizontal movement. Normal forces (applied load) were estimated from force–displacement curves, where $F_N = 0$ is taken to be the value just before the jump to contact. The surfaces were not modified by scanning at high applied loads.

Friction force measurements [25] were performed on a single scan line (scan distance 2 μm) at low scanning speed (1–5 μm/s). Differences in humidity, chemical nature of the tip (adsorbed species from the lab atmosphere) and the alignment of the laser on the cantilever changes the magnitude of F_f [26]. Therefore, care was taken to minimise the influence of these parameters by measuring in a humidity-controlled room. Furthermore, all F_f versus F_N curves in each figure were taken on the same day and with the same tip without changing the alignment. Despite these precautions, absolute values for the friction coefficient cannot be deduced from our measurements.

3. Results

3.1. AFM and LFM

In Fig. 1, some snapshots of the time evolution of the formation of a self-assembled monolayer composed of octadecyltrichlorosilane (OTS) on $SrTiO_3$ are shown. Before adsorption, an atomically smooth surface is visible with terraces (width is approx. 100–150 nm, in accordance with the miscut angle of the substrate, Fig. 1a). After 10 s of immersion in the solution, the topography distinctly changes (Fig. 1b). Two types of islands appear: type I is 'fractal-like' shaped and quite large, whereas type II is more circularly shaped and smaller (diameter about 50 nm). Longer immersion times result in a reduction of both the number and size of the 'fractals', and in an increase of the size and a change of the shape of the type II islands. After t = 10 min (Fig. 1c) only few 'fractal-shaped' islands have survived, leaving the remaining surface to consist of interconnected, irregularly shaped islands. The formation of the SAM is completed for $t \geq 60$ min (Fig. 1d). Immersion for even longer times only results in a slightly more densely

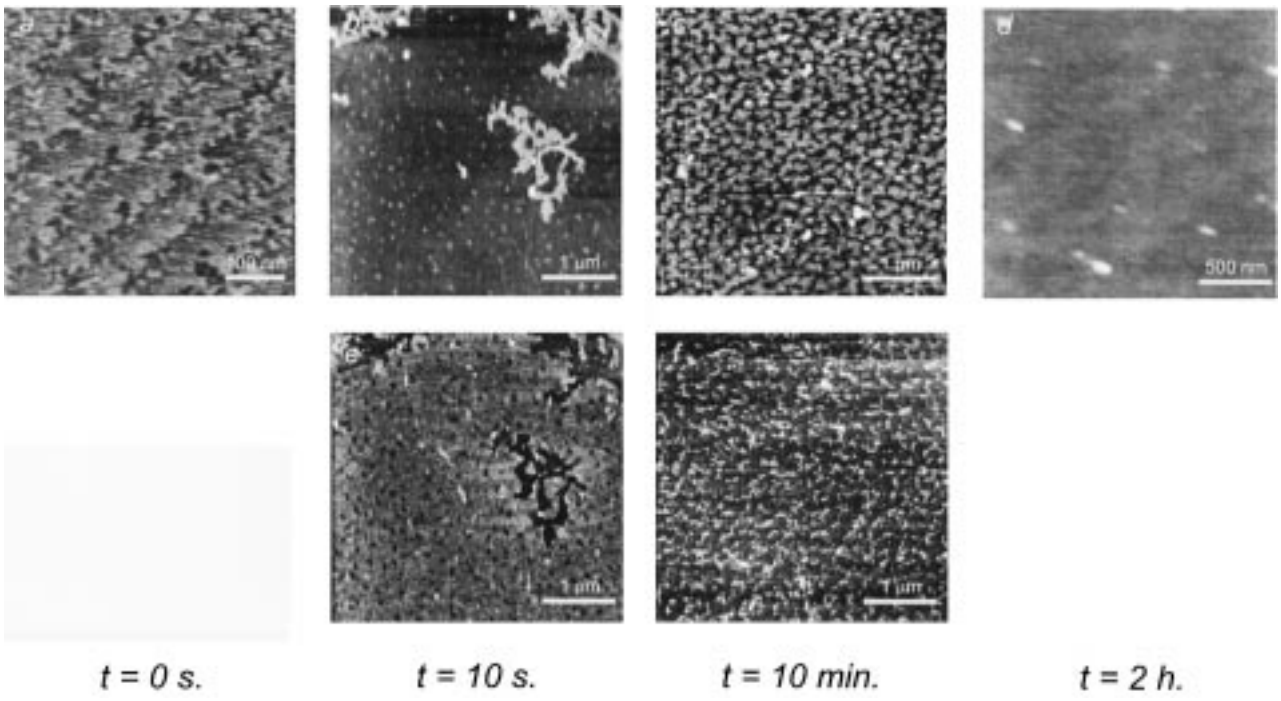

Fig. 1. Atomic force micrographs of OTS on $SrTiO_3$-surfaces at different adsorption times: (a) 0 s, (b) 10 s, (c) 10 min, (d) 120 min, (e) lateral force micrograph of area in b, and (f) lateral force micrograph of area in c. The grey-scale for the LFM micrographs ranges from lower to higher frictional forces exerted on the cantilever.

packed monolayer and in the formation of lamellae (bilayers) on top of the first monolayer [19].

Simultaneously, lateral force micrographs were recorded (see Fig. 1e (t = 10 s) and Fig. 1f (t = 10 min)). It is clearly visible that both types of islands exert lower friction on the cantilever than the substrate; however, also parts with higher friction are visible. Friction vs. applied load curves were measured as well. For all samples, the measured friction F_f increases linearly with applied load F_N, i.e. $F_f = F_{f0} + \mu F_N$, where μ is termed the friction coefficient [25]. Some examples are shown in Fig. 2a. The bare $SrTiO_3$ substrate has the highest μ (as evidenced by the steepest slope), and a completed methyl-terminated SAM the lowest. Little difference exists between OTS–$SrTiO_3$ and OTS–$SrTiO_3$:Nb.

All curves were measured on a 2-μm long scan line, averaging over all features present. Zooming in on, e.g. a fractal-shaped island, a value for μ is found close to that of a completed crystalline SAM. In this case, the measured μ does not yield a reliable value; therefore, μ (t = 10 s) has been omitted. Fig. 2b summarises the results obtained for the friction coefficient μ as a function of immersion time t.

3.2. Wettability

Advancing and receding contact angles (CAs) of water

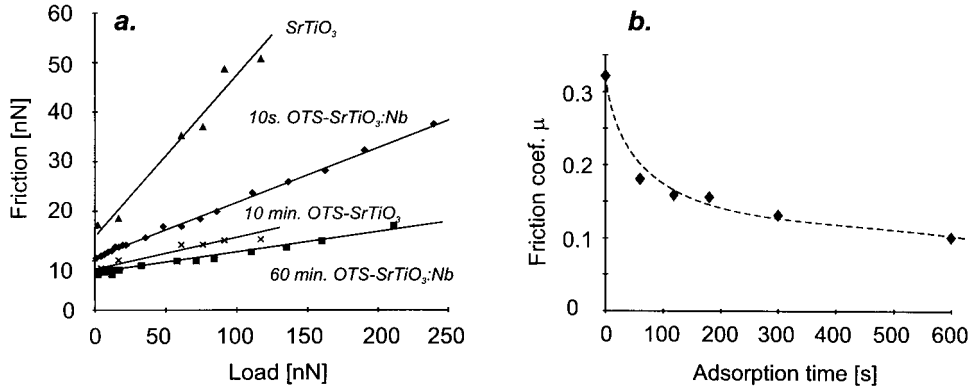

Fig. 2. (a) Friction versus applied load curves at different adsorption times. The solid lines are linear fits to the data points. (b) Friction coefficient μ as a function of immersion time t for OTS on $SrTiO_3$ (the dashed curve serves as a guide to the eye). The used tip had nominal force constants k_N = 0.38 and k_{tors} = 80 N/m [24].

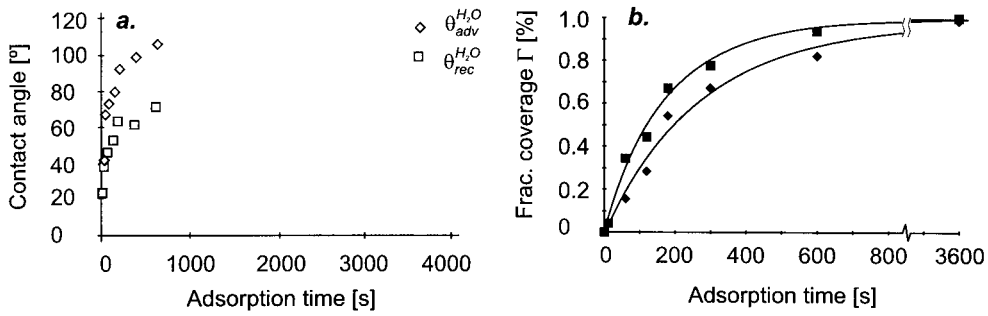

Fig. 3. (a) Advancing and receding contact angles of water on partial SAMs of OTS on $SrTiO_3$. (b) Fractional surface coverage of OTS islands on a $SrTiO_3$-surface as a function of the immersion time t; (♦) is calculated by Eq. (1) from the wettability data, and (■) is calculated from the AFM topographs. The solid curves are fits of the first-order Langmuir isotherm to the data (see text for details). Note the discontinuity in the time-axis.

were measured immediately after formation of all SAMs. Clean $SrTiO_3$-surfaces exhibit an advancing CA of water of approx. 40°, whereas a completed OTS-monolayer (formed after immersion times longer than 1 h) is hydrophobic with $\theta^{H_2O}_{adv}$ = 115° (θ^{HD}_{adv} = 44°) [19]. The samples immersed for intermediate periods of time also had intermediate CAs (Fig. 3a). To fit the data by an isotherm, the fractional coverage of OTS-islands on the $SrTiO_3$ surface is calculated. Based on Cassie's equation [16], the equilibrium contact angle for heterogeneous films consisting of microscopic domains of OTS (with contact angle θ_1 and fractional coverage Γ_1) on bare $SrTiO_3$ (with contact angle θ_2 and fractional coverage $1-\Gamma_1$) can be expressed as

$$\cos\theta^{H_2O}_{adv} = \Gamma_1\cos\theta_1 + (1-\Gamma_1)\cos\theta_2 \quad (1)$$

These values can be compared to the coverage as determined by the AFM topographs.[1] The fractional coverage data can then be fitted by a simple first-order Langmuir isotherm. This model assumes that OTS molecules adsorb randomly (i.e. there is no site-specificity for adsorption [21]) and that they have no interaction with each other

$$\Gamma = \Gamma_{max}(1-\exp(-k_{obs}t)) \quad (2)$$

where Γ_{max} is the maximum fractional coverage and kobs the observed reaction rate. In Fig. 3b, the fits are shown and its parameters are summarised in Table 1.

4. Discussion

It is evident from the AFM micrographs that as early as the first few seconds OTS nucleates as islands on the surface of $SrTiO_3$. The height of these islands is approximately 2.1–2.3 nm, slightly less than the thickness of a completed SAM [14,17–19]. From the friction measurements, it can be seen that the structure of these 'fractal-shaped' islands is already close to the final SAM structure in terms of packing density and crystallinity. Presumably, these islands are formed in the solution and physisorbed onto the water film present on the $SrTiO_3$ substrate. Growth occurs via the competing process of adsorption and desorption of individual molecules (or more precisely, a small number of molecules) at random sites on the surface. These small patches act as a nucleation site, but they can also migrate and attach to other islands. The thickness of these patches ranges from 0.8 to 1.2 nm, indicating a high tilt angle and loose packing. It cannot be ruled out, however, that during growth, more molecules are present on the water film covering the surface. These monomers could have been removed during rinsing with chloroform, and are therefore not visible by AFM. Islands and patches could grow by attachment of these molecules [10]. Subsequent adsorption of more 'fractal-like' islands would be hindered by the presence of these monomers, which is in accordance with what we have observed. Such hindrance is more pronounced for longer than for shorter alkylchains [17]. The bright spots visible in the height (Fig. 1b,c) and friction micrographs (Fig. 1e,f) are attributed to impurities with a different chemical nature than the surrounding OTS or $SrTiO_3$, since they have a different frictional contrast.

Close analogies exist between the growth of OTS on $SrTiO_3$, SiO_2 [18] and mica [12–14], and a Langmuir monolayer [18,22]. In the phase diagram of an insoluble surfactant on the air–water interface (Langmuir films) coexistence regions exist as a function of the compression of the molecules. At low compression (i.e. high area per molecule) the

[1] Two possibilities exist to measure surface coverage. The first method is to convert the greyscale image to a binary image (by the grain size analysis routine of the Nanoscope software), and count the number of pixels belonging to islands and divide this number by the total amount of pixels. Another method is to plot the number of pixels of each 'colour' of grey in a histogram. The result can be identified as the envelope of two Gaussian curves, one centred around the darker pixels and one centred around lighter pixels. Again, the fractional coverage is the area under the second Gaussian divided by the total number of pixels. We have employed the first method.

Table 1

Summary of fit parameters for the fractional coverage data with Eq. (2)

	$SrTiO_3$ (CA)	$SrTiO_3$ (AFM)	$SrTiO_3$:Nb (CA)
Γ_{max} (%)	0.98	0.98	0.86
k_{obs} (s^{-1})	3.6×10^{-3}	5.7×10^{-3}	1.4×10^{-3}

molecules are in a gas phase (G), and, upon increasing the compression, the phase alters via liquid expanded (LE) to liquid condensed (LC). In the G- and LE-phases, the molecules contain a large number of gauche defects, whereas the molecules in the LC-phase are mainly in an all-*trans* conformation. At higher adsorption temperatures, these phases are not separated, but G/LE and LE/LC coexistence regions exist, resulting in lower packing density and more 'liquid-like' films. If this description is used for SAMs, the existence of a critical temperature T_c for the formation of high quality films can be explained. Below T_c, no coexistence regions are present, and only crystalline (LC*) films are formed.[2] Above T_c, however, the presence of the LE*/LC* region results in more liquid-like SAMs [18]. For OTS, T_c ranges from 23° to 32°C [22,23],[3] depending on the measurement technique.

For alkyltrichlorosilane SAMs on oxidic substrates, our results can be explained by a similar phase diagram. The 'fractal-like' islands are densely packed and in an all-*trans* conformation, as indicated by their thickness and friction coefficient, and can therefore be considered as domains of the LC* phase. The smaller circular patches are more liquid-like, as seen from their thickness and frictional behaviour, and are said to be in the LE* phase. Therefore, in this picture, the surface pressure increases for increasing number of adsorbed molecular patches, which in turn increases the crystallinity of the SAM. If the temperature during assembly is kept below T_c, as is the case in our experiments, the monolayer will finally be crystalline (LC* phase).

The friction coefficient shows the same general behaviour as the wettability data (compare Fig. 2 and 3a)[4] and can be described by a first-order Langmuir isotherm (Eq. (2)). Although the AFM micrographs already indicate nearly complete coverage, the friction coefficient has not yet reached its lowest value. A possible reason for this is that the tip-sample contact area is higher (i.e. the tip penetrates the monolayer), because the monolayer is not yet densely packed and will therefore increase the frictional force [28].

The wettability data, combined with the AFM fractional coverage data, suggest a similar picture. The assumption that there is a two-phase system (i.e. the substrate and one OTS phase) is too simple. As is evident from Fig. 3b, the coverage as calculated by Eq. (1) yields smaller values. The reason for this discrepancy is that not all OTS-islands are as crystalline and densely packed as the 'fractal-like' islands. It would be more appropriate to introduce a third phase. However, the implementation of this idea is not trivial, since the LE*-phase is continuously changing to the LC*-phase.

The growth mechanism of OTS on $SrTiO_3$ (and $SrTiO_3$:Nb) and SiO_2 are remarkably similar. Growth of SAMs comprised of alkyltrichlorosilanes on both substrates proceeds via the nucleation of islands, which serve as a nucleation centre for mobile patches. The patches also grow by attachment of monomers. This correspondence of the growth behaviour on these widely different substrates is another indication that the film structure is decoupled from substrate properties as chemical identity of surface species and its lattice parameters. One important parameter that remains is the surface hydration. Furthermore, such a general mechanism may provide a general strategy for the formation of high quality alkylsiloxane SAMs on many different oxidic substrates. The observed rate constant k_{obs} is in good agreement with other reports. Flinn et al. [10] reports a somewhat smaller and concentration-dependent rate of $1.90C - 2.31 \times 10^{-5}$ (with concentration $C = 1$ mM, $k_{obs} = 1.9 \times 10^{-3}$). No other direct rates have been given, but from the data (thickness and wettability) given by Bierbaum et al., a rate $k_{obs} \sim 1 \times 10^{-3}$ and 5×10^{-3}, respectively, can be obtained [17]. For thiols on gold, much faster rates have been determined ($k_{obs} \sim 1\text{–}100 \times 10^{-2}$ [6–8]), depending on chain length, solvent and concentration.

The main difference observed in this study between $SrTiO_3$ and $SrTiO_3$:Nb substrates is that the growth rate appears to be lower on the niobium-doped surface (see Table 1). Furthermore, from previous studies it can be concluded that the tilt angles of OTS molecules is larger on the latter substrate.

5. Conclusion

It has been shown that growth of self-assembled monolayers of OTS on $SrTiO_3$ proceeds via the adsorption of crystalline 'fractal-shaped' islands and more 'liquid-like' patches of molecules. These islands grow via attachment of other patches and/or molecules, thereby increasing their packing density and crystallinity. This growth mechanism is similar to that found for OTS on SiO_2, and agrees with a model of a Langmuir monolayer on a water surface. The overall growth mechanism can be described by a first-order Langmuir isotherm, in which the growth rate is proportional to the number of unoccupied surface sites. The main difference between $SrTiO_3$ and $SrTiO_3$:Nb is that the latter SAM forms slightly slower. Measurements of lateral forces are a powerful additional technique for comparing different samples, but care must be taken to ensure identical conditions during friction measurements, since they might influence the results.

[2] The superscript * denotes phases in the SAM.

[3] Recently, another view on the existence of a T_c was presented by Rye. It was suggested that the interplay between the thermal and alkane–alkane interaction energy could be such, that above T_c (associated with the alkane melting transition) the chains are disordered and that these chains block (or sterically hinder) the adsorption of a sufficient number of new molecules to generate a densely packed crystalline SAM. However, the analogy between Langmuir monolayers and OTS growth is found to be useful to describe the formation mechanism [27].

[4] The shape of the adhesion force versus adsorption time displays the same trend as the curve of the friction coefficient. The initial adhesion on a clean surface is high, but already after an immersion of 10 s, the adhesion force decreases considerably.

References

[1] A. Ulman, An Introduction to Ultrathin Organic Films, From Langmuir–Blodgett to Self-Assembly, Academic Press, San Diego, CA, 1991.
[2] A. Ulman, Chem. Rev. 96 (1996) 1533.
[3] M. Kawasaki, A. Ohtomo, T. Arakane, K. Takahashi, M. Yoshimoto, H. Koinuma, Appl. Surf. Sci. 107 (1996) 102.
[4] C.D. Bain, G.M. Whitesides, J. Am. Chem. Soc. 111 (1989) 7164.
[5] C.D. Bain, E.B. Troughton, Y.-T. Tao, J. Evall, G.M. Whitesides, R.G. Nuzzo, J. Am. Chem. Soc. 111 (1989) 321.
[6] M. Buck, F. Eisert, J. Fischer, M. Grunze, F. Träger, Appl. Phys A 53 (1991) 552.
[7] D.S. Karpovich, G.J. Blanchard, Langmuir 10 (1994) 3315.
[8] K.A. Peterlinz, R. Georgiadis, Langmuir 12 (1996) 4731.
[9] G.E. Poirier, E.D. Pylant, Science 272 (1996) 1145.
[10] J.T. Woodward, D.K. Schwartz, J. Am. Chem. Soc. 118 (1996) 7861.
[11] X.-D. Xiao, G.-Y. Liu, D.H. Charych, M. Salmeron, Langmuir 11 (1995) 1600.
[12] D.K. Schwartz, S. Steinberg, J. Israelachvili, J.A.N. Zasadzinski, Phys. Rev. Lett. 69 (1992) 2254.
[13] J.A. Zasadzinski, R. Viswanathan, D.K. Schwartz, J. Garnaes, L. Madsen, S. Chiruvolu, J.T. Woodward, M.L. Longo, Colloid Surf. A 93 (1994) 305.
[14] D.W. Britt, V. Hlady, J. Colloid Interface Sci. 178 (1996) 775.
[15] A. Barrat, P. Silberzan, L. Bourdieu, D. Chatenay, Europhys. Lett. 20 (1992) 633.
[16] D.H. Flinn, D.A. Guzonas, R.-H. Yoon, Colloid Surf. A 87 (1994) 163.
[17] K. Bierbaum, M. Grunze, A.A. Baski, L.F. Chi, W. Schrepp, H. Fuchs, Langmuir 11 (1995) 2143.
[18] J.V. Davidovits, V. Pho, P. Silberzan, M. Goldmann, Surf. Sci. 352-354 (1996) 369.
[19] B.L. Kropman, D.H.A. Blank, H. Rogalla, Supramol. Sci. 4 (1997) 59.
[20] B.L. Kropman, D.H.A. Blank, H. Rogalla, Mater. Sci. Eng. C 5 (1998) 163.
[21] X. Zhao, R. Kopelman, J. Phys. Chem. 100 (1996) 11014.
[22] J.B. Brzoska, I. Ben Azouz, F. Rondelez, Langmuir 10 (1994) 4367.
[23] A.N. Parikh, D.L. Allara, I. Ben Azouz, F. Rondelez, J. Phys. Chem. 98 (1994) 7577.
[24] A. Noy, C.D. Frisbie, L.F. Rozsnyai, M.S. Wrighton, C.M. Lieber, J. Am. Chem. Soc. 117 (1995) 7943.
[25] E. Meyer, R. Overney, D. Brodbeck, L. Howald, R. Lüthi, J. Frommer, H.-J. Güntherodt, Phys. Rev. Lett. 69 (1992) 1777.
[26] J. Hu, X.-D. Xiao, D.F. Ogletree, M. Salmeron, Surf. Sci. 327 (1995) 358.
[27] R.R. Rye, Langmuir 13 (1997) 2588.
[28] G. Bar, S. Rubin, A.N. Parikh, B.I. Swanson, T.A.Zawodzinski Jr., M.-H. Whangbo, Langmuir 13 (1997) 373.